Electronic Supplementary Information

Graphene nanoribbons blends with P3HT for organic electronics

Mirella El Gemayel,[a] Akimitsu Narita,[b] Lukas F. Dössel,[b] Ravi Shankar Sundaram,[c] Adam Kiersnowski,[b,d] Wojciech Pisula,[b] Michael Ryan Hansen,[b,e] Andrea C. Ferrari,[c] Emanuele Orgiu,[a] Xinliang Feng [b,]Klaus Müllen,[b,*], Paolo Samorì[a,*]*

[a] Nanochemistry Laboratory, ISIS & icFRC, Université de Strasbourg & CNRS, 8 allée Gaspard Monge, 67000 Strasbourg, France

[b] Max-Planck Institute for Polymer Research, Ackermannweg 10, 55124 Mainz, Germany.

[c] Cambridge Graphene Center, Department of Engineering, Cambridge University, 9 JJ Thomson Avenue, Cambridge CB3 OFA, UK

[d] Polymer Engineering and Technology Division Wroclaw University of Technology Wybrzeze Wyspianskiego 27, 50-370 Wroclaw, Poland.

[e] Interdisciplinary Nanoscience Center (iNANO) and Department of Chemistry, Aarhus University, Gustav Wieds Vej 14, DK-8000 Aarhus C, Denmark.

E-mail: samori@unistra.fr, muellen@mpip-mainz.mpg.de, feng@mpip-mainz.mpg.de

Table of Contents

1. Instrumentation and characterization

All reactions dealing with air- or moisture-sensitive compounds were carried out in a dry reaction vessel under argon. Microwave-assisted reactions were performed using a CEM microwave reactor Discover-S-Class. Preparative column chromatography was performed on silica gel from Merck with a grain size of 0.063–0.200 mm (silica gel) or 0.04–0.063 mm (flash silica gel, Geduran Si 60). Both analytical and preparative thin layer chromatography (TLC) was performed on silica gel coated substrates "60 F254" from Merck. ^{1}H and ^{13}C NMR spectra were recorded on Bruker DPX250, AMX300, DRX500, and DRX700, and referenced to residual signals of the deuterated solvent. Abbreviations: s = singlet, d = doublet, t = triplet, m = multiplet. Field desorption mass spectra (FD/MS) were obtained with a VG Instruments ZAB 2-SE-FDP using 8 kV accelerating voltage. The high-resolution mass spectrometry was performed on an ESI-Q-TOF system (maXis, BrukerDaltonics, Germany). The instrument was operated in wide pass quadrupole mode, for MS experiments, with the TOF data being collected between m/z 100–5000. Matrix-assisted laser desorption/ionization time-of-flight (MALDI-TOF) mass spectra were recorded using a Bruker Reflex II utilizing a 337 nm nitrogen laser, calibrated against poly(ethylene glycol) (3000 g/mol). Elemental analysis of solid samples was carried out on a Foss Heraeus Vario EL. Analytical gel permeation chromatography (GPC) was performed on SDV PSS GPC columns using THF as eluent at a temperature of 303 K. The refractive index was determined on a RI ERC 7512 detector (ERMA). Infrared spectroscopy was measured on a Nicolet 730 FT-IR spectrometer equipped with an attenuated total reflection (ATR) setup. The samples were deposited as pristine material on the diamond crystal and pressed on it with a stamp. Measurements with a scan number of 128 were recorded for each sample and the background was subtracted.

2. Synthesis and analysis

2,5-Di([1,1'-biphenyl]-3-yl)-3,4-bis(4-dodecylphenyl)cyclopenta-2,4-dienone (S3)

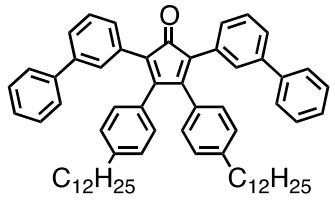

To a degassed solution of 4,4'-didodecylbenzil (**S2**)[1] (400 mg, 0.731 mmol) and 1,3-di(biphenyl-3-yl)propan-2-on (**1**) (265 mg, 0.731 mmol) in *tert*-butanol (10 mL) was added at 80 °C a methanol solution of tetrabutylammonium hydroxide (1.00 M, 1.10 ml, 1.10 mmol). After stirring at 80 °C for 20 min the reaction was quenched with water, and the reaction mixture was extracted three times with dichloromethane. The combined organic layers were washed with brine three times, dried over sodium sulfate, and evaporated to give a purple crude product. Purification by silica gel column chromatography (eluent: 20–25% toluene/hexane) gave the title compound as a purple solid (420 mg, 0.481 mmol, 66% yield): Mp: 77–78 °C; ^{1}H NMR (300 MHz, CD_2Cl_2) δ = 7.48 (dt, J = 6.9, 1.9 Hz, 2H, CH), 7.44–7.26 (m, 16H, CH), 7.07 (d, J = 8.1 Hz, 4H, CH), 6.94 (d, J = 8.1 Hz, 4H, CH), 2.61 (t, J = 7.4 Hz, 4H, α-CH_2), 1.69–1.56 (m, 4H, β-CH_2), 1.40–1.23 (br m, 36H, -CH_2-), 0.89 (t, J = 6.9 Hz, 6H, -CH_3); ^{13}C NMR (75 MHz, CD_2Cl_2) δ = 200.69, 155.82, 144.34, 141.25, 141.02, 132.05, 131.02, 129.74, 129.46, 129.39, 129.07, 128.88, 128.51, 127.64, 127.36, 126.39, 125.40, 36.23, 32.38, 31.91, 30.15, 30.13, 30.11, 30.08, 29.95, 29.82, 29.75, 23.14, 14.32; MS (MALDI-TOF, positive): m/z: 873.8 [M^+] (calcd. for $C_{65}H_{76}O$: 872.6); Rf (20% toluene/hexane) = 0.15.

1,4-Bis(biphenyl-3-yl)-2,3,4,5-tetrakis(4-dodecylphenyl)-benzene (S4)

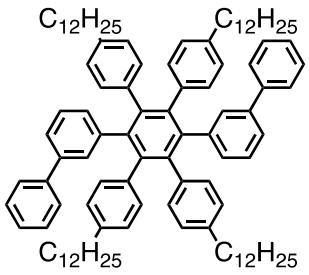

A degassed solution of 2,5-di([1,1'-biphenyl]-3-yl)-3,4-bis(4-dodecylphenyl)cyclopenta-2,4-dienone (**S3**) (300 mg, 0.344 mmol) and bis(4-dodecylphenyl)acetylene[2] (178 mg, 0.346 mmol) in diphenyl ether (2.0 mL) was refluxed for 110 h by using a heating mantle. After cooling down to room temperature the reaction mixture was diluted with hexane and purified by silica gel column chromatography (eluent: 10% dichloromethane/hexane) to give the title compound as a pale yellow solid (277 mg, 0.204 mmol, 59% yield): Mp: 103.6 °C; ^{1}H NMR (700 MHz, CD_2Cl_2) δ = 7.32–7.27 (m, 4H, CH), 7.25–7.21 (m, 2H, CH), 7.16 (t, J = 7.2 Hz, 4H, CH), 7.09–7.05 (m, 4H, CH), 6.93 (td, J = 7.6, 2.5 Hz, 2H, CH), 6.82 (d, J = 7.8 Hz, 4H, CH), 6.80 (d, J = 7.9 Hz, 2H, CH), 6.76 (d, J = 7.8 Hz, 2H, CH), 6.75–6.70 (m, 6H, CH), 6.68 (t, J = 8.4 Hz, 4H, CH), 2.39–2.31 (m, 8H, α-CH_2), 1.41–1.33 (m, 8H, β-CH_2), 1.33–1.12 (m, 64H, -CH_2-), 1.11–1.04 (m, 8H, -CH_2-), 0.88 (t, J = 7.0 Hz, 12H, -CH_3); ^{13}C NMR (75 MHz, CD_2Cl_2) δ = 141.83, 141.72, 140.92, 140.77, 140.20, 139.71, 138.67, 131.92, 131.72, 131.24, 131.03, 128.84, 127.35, 127.27, 127.14, 127.08, 124.13, 35.75, 32.40, 31.74, 30.17, 30.13, 30.09, 29.93, 29.84, 29.34, 23.15, 14.33; MS (MALDI-TOF, positive): m/z: 1359.2 [M^+] (calcd. for $C_{102}H_{134}$: 1360.1); Rf (10% dichloromethane/hexane) = 0.27.

PAHs S5 and S6

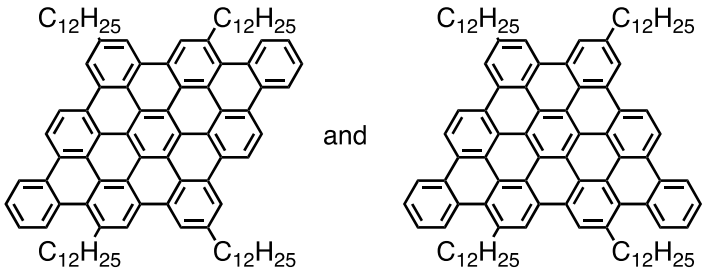

A solution of 1,4-bis(biphenyl-3-yl)-2,3,4,5-tetrakis(4-dodecylphenyl)-benzene (**S4**) (99.8 mg, 73.4 μmol) in unstabilized dichloromethane (30 mL) was degassed by argon bubbling for 15 min. To the solution was added a suspension of iron (III) chloride (581 mg, 3.58 mmol) in nitromethane (2.0 mL). After stirring at room temperature for 3 h with a continuous argon flow through the reaction mixture, the reaction was quenched by the addition of methanol to form dark yellow powder. Filtration and washing intensively with methanol to gave the title compounds as dark yellow powder (71.4 mg, 51.1 μmol, 72% yield): Mp: >320 °C; ^{1}H NMR (500 MHz, 1,1,2,2-tetrachloroethane-d_2, 393 K) δ = 9.11–8.65 (m, 8H, CH), 8.56 (m, 2H, CH), 8.49–8.10 (m, 4H, CH), 8.04–7.78 (m, 4H, CH), 3.91–3.78 (m, 2H, α-CH_2), 3.77–3.61 (m, 2H, α-CH_2), 3.30–3.14 (m, 2H, α-CH_2), 3.14–3.02 (m, 2H, α-CH_2), 2.37–2.01 (m, 8H, β-CH_2), 1.97–1.18 (m, 72H, -CH_2-), 1.15–0.82 (m, 12H, -CH_3); ^{13}C NMR could not be recorded due to strong aggregation of the compound in the solution even at elevated temperature or diluted conditions[3]; MS (MALDI-TOF, positive): *m*/*z*:1344 [M^+] (calcd. for $C_{102}H_{118}$: 1344).

^{1}H and ^{13}C NMR Spectra

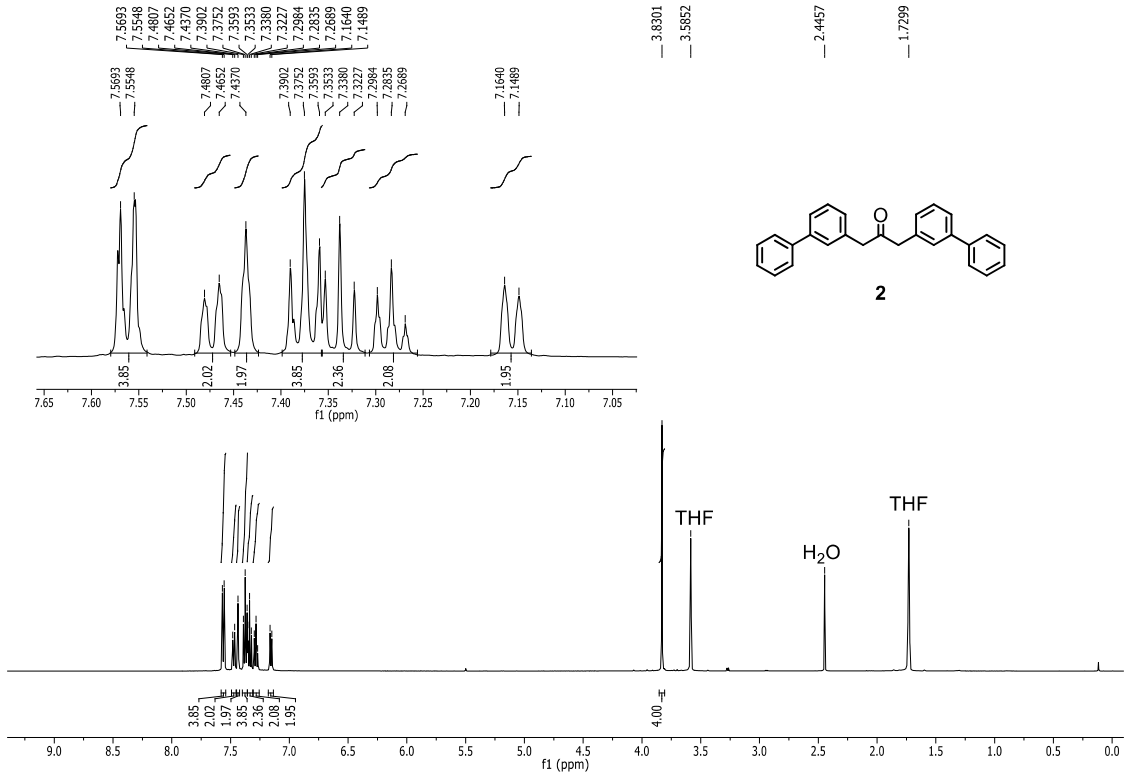

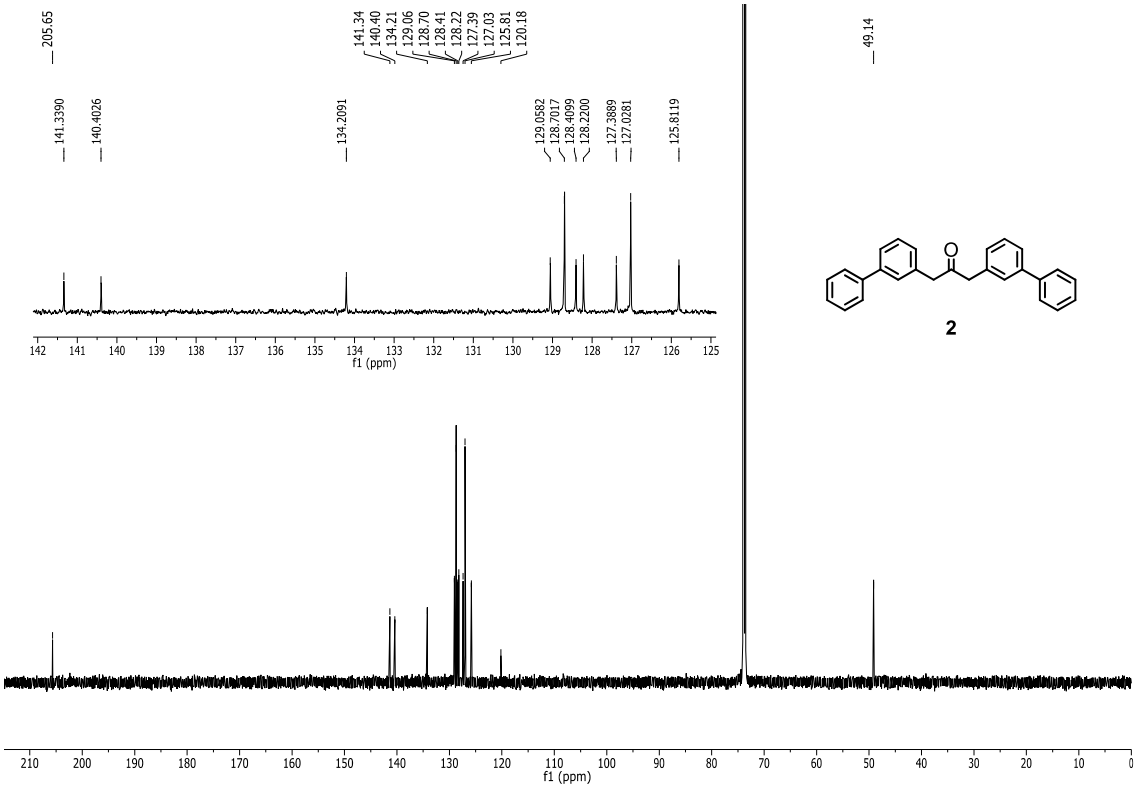

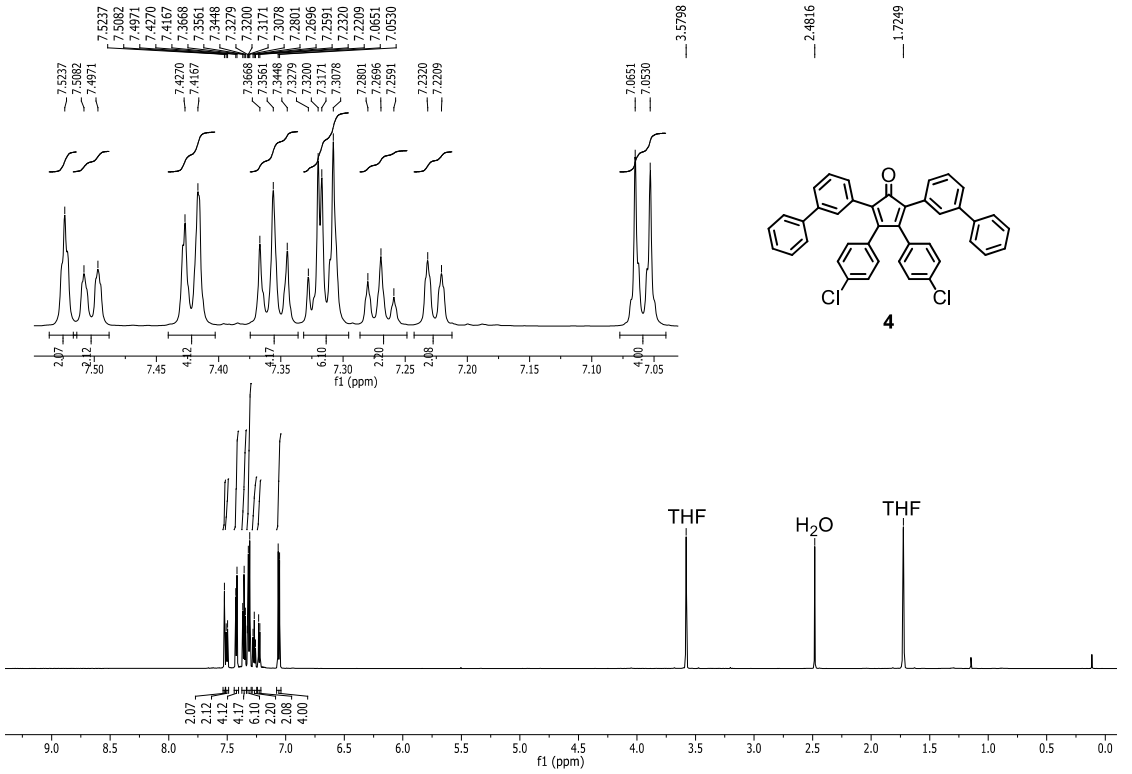
7.5237
7.5082
7.4971
7.4270
7.4167
7.3668
7.3561
7.3448
7.3279
7.3200
7.3171
7.3078
7.2801
7.2696
7.2591
7.2320
7.2209
7.0651
7.0530
3.5798
2.4816
1.7749
O
Cl
Cl
4
THF
H2O
THF
f1 (ppm)

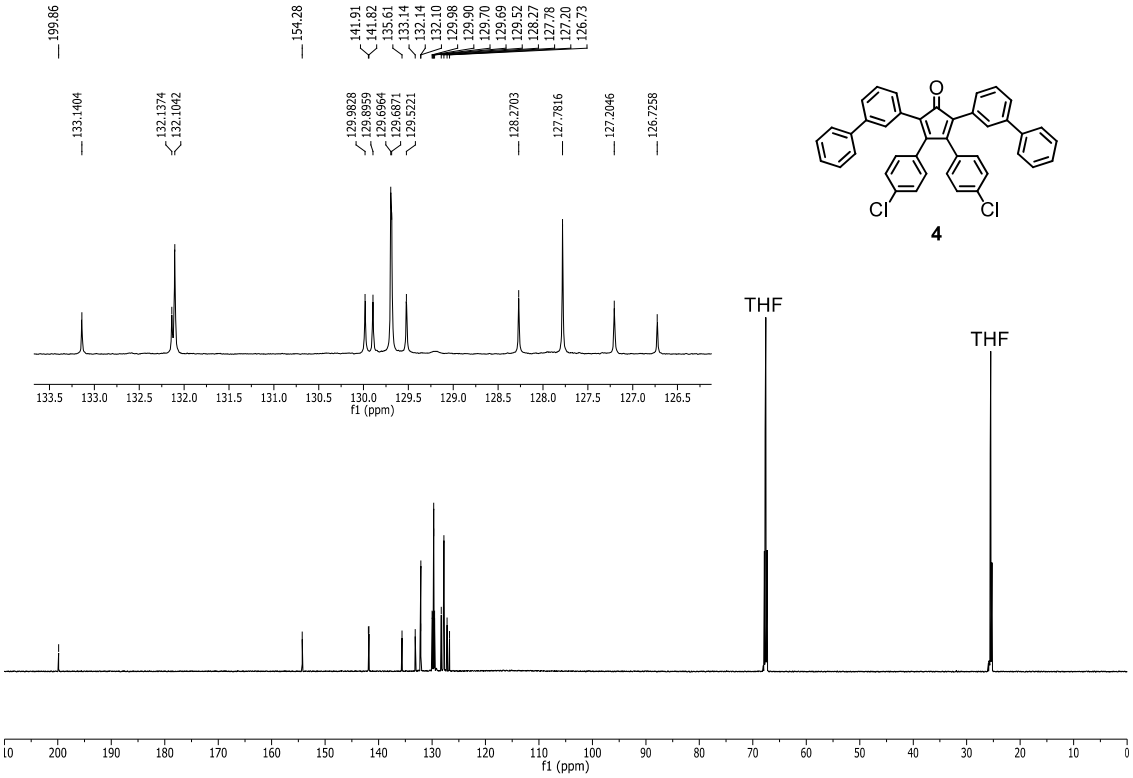
199.86
154.28
141.91
141.82
135.61
133.14
132.14
132.10
129.98
129.90
129.70
129.69
129.52
128.27
127.78
127.20
126.73
133.1404
132.1374
132.1042
129.9828
129.8959
129.6964
129.6871
129.5221
128.2703
127.7816
127.2046
126.7258
O
Cl
Cl
4
THF
THF
f1 (ppm)

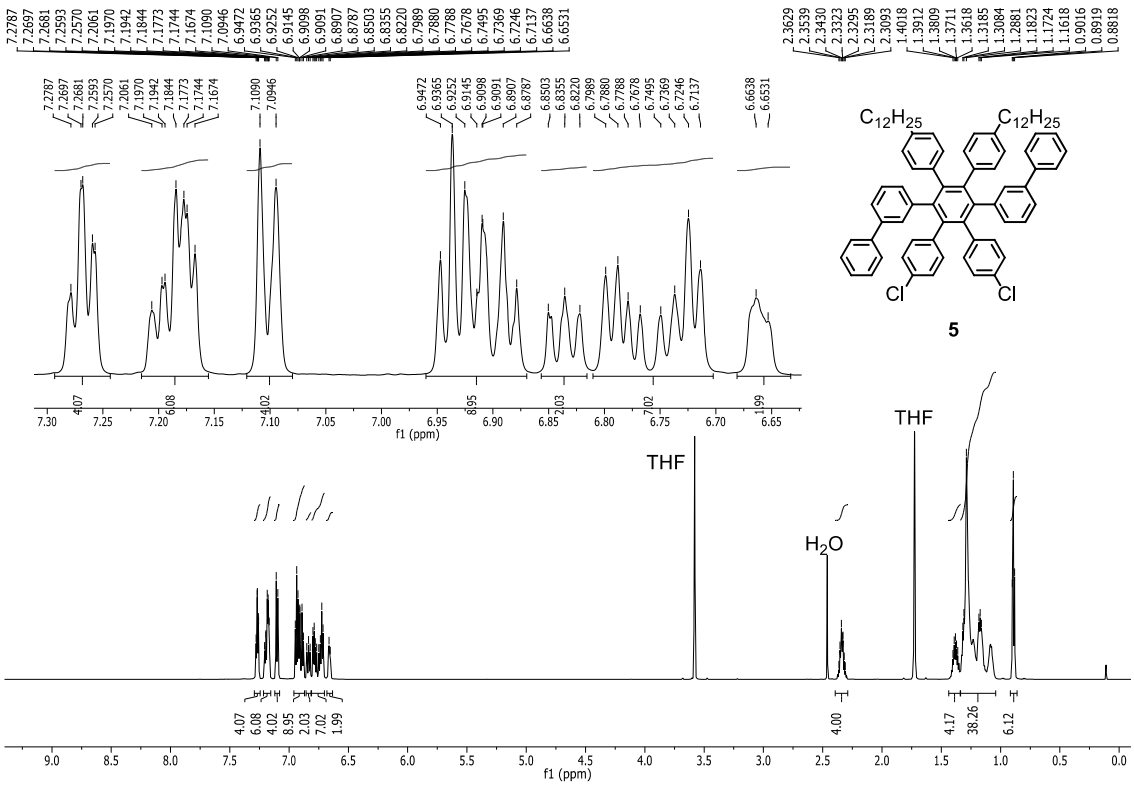
THF
H2O
THF
f1 (ppm)

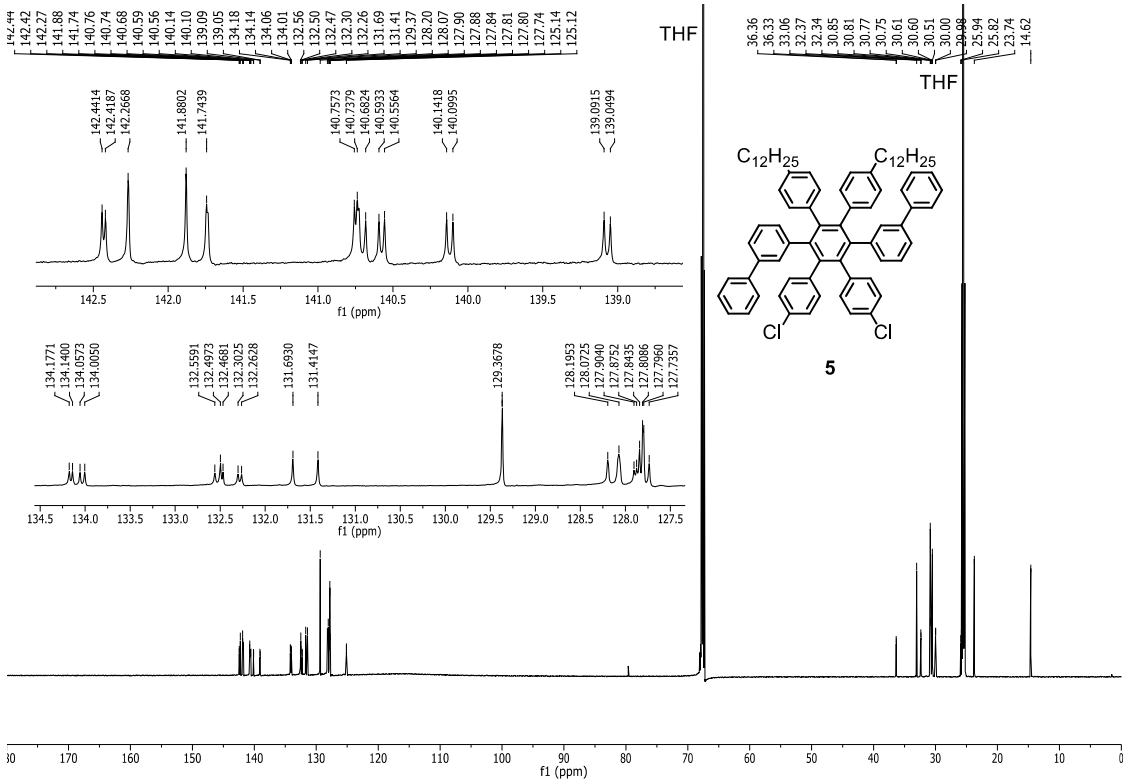
THF
THF
f1 (ppm)

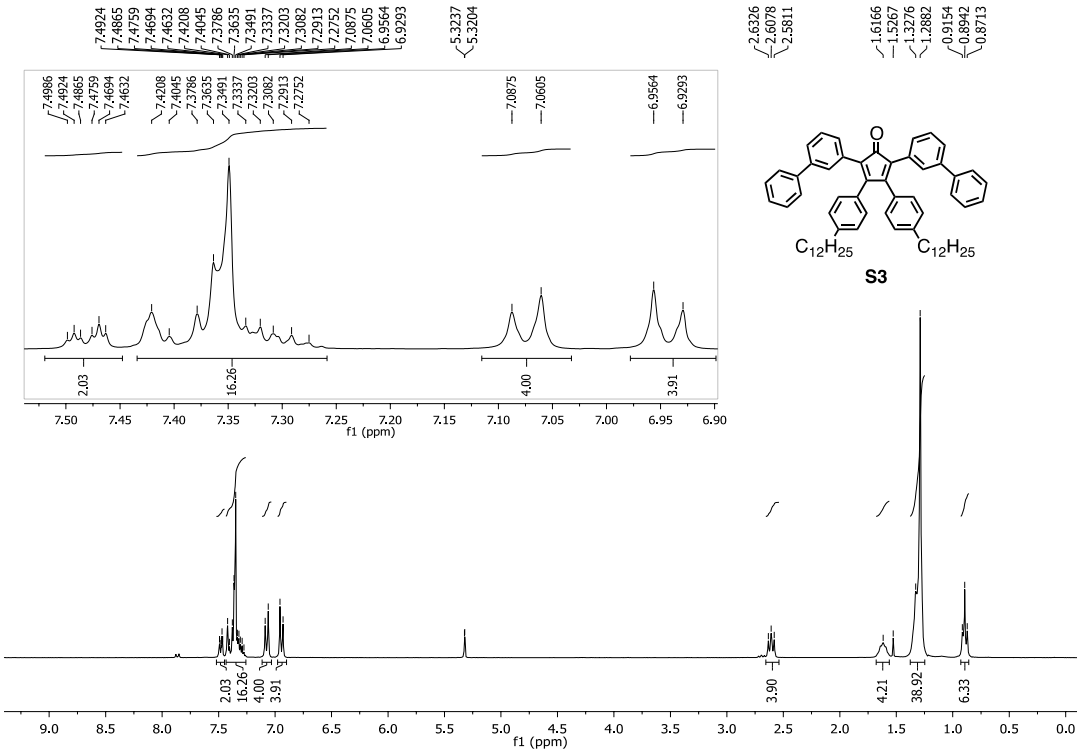
S3

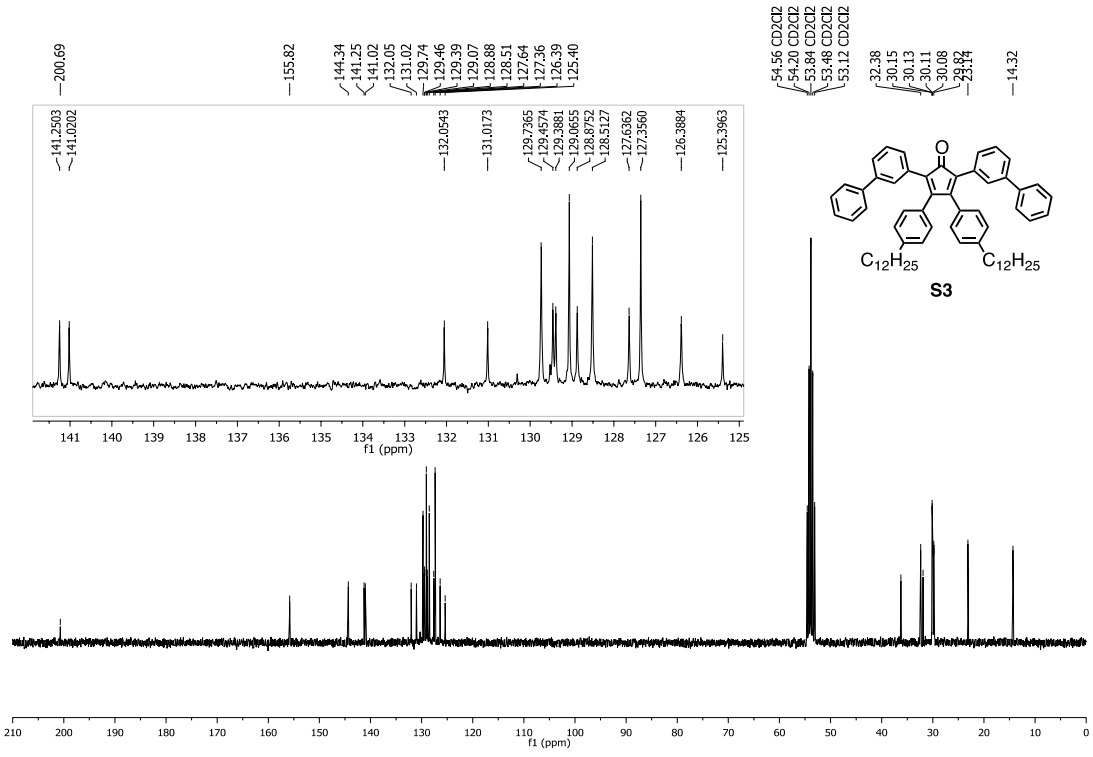
S3

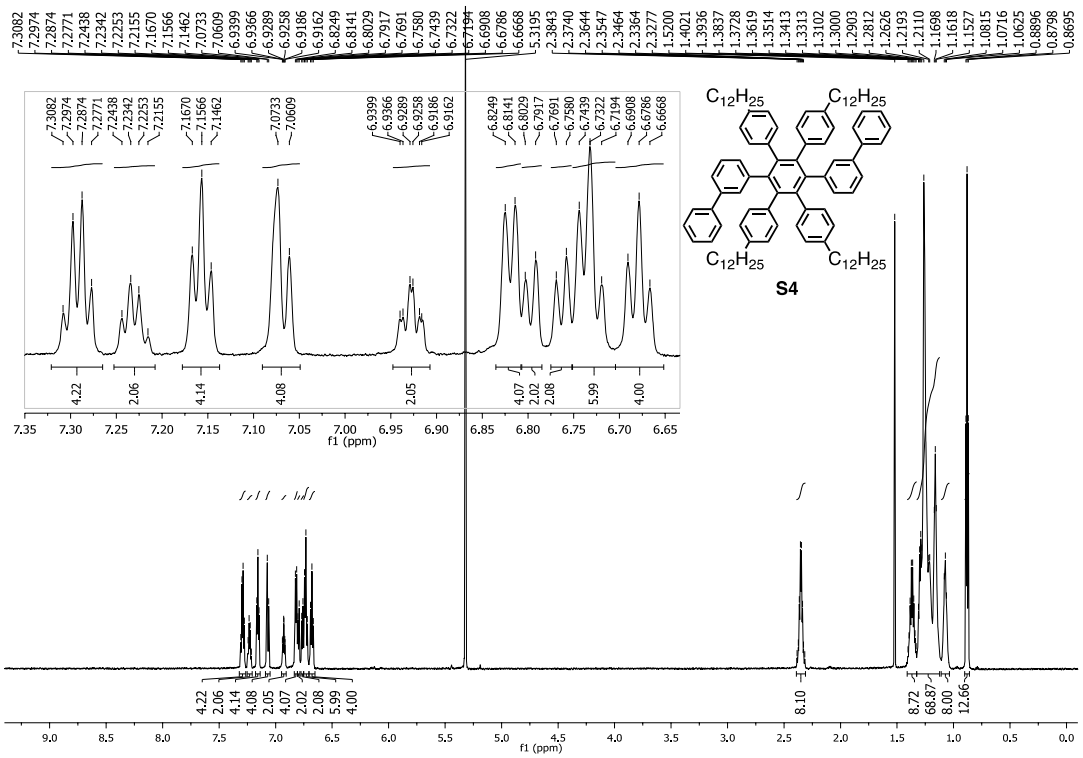
C12H25
S4
f1 (ppm)

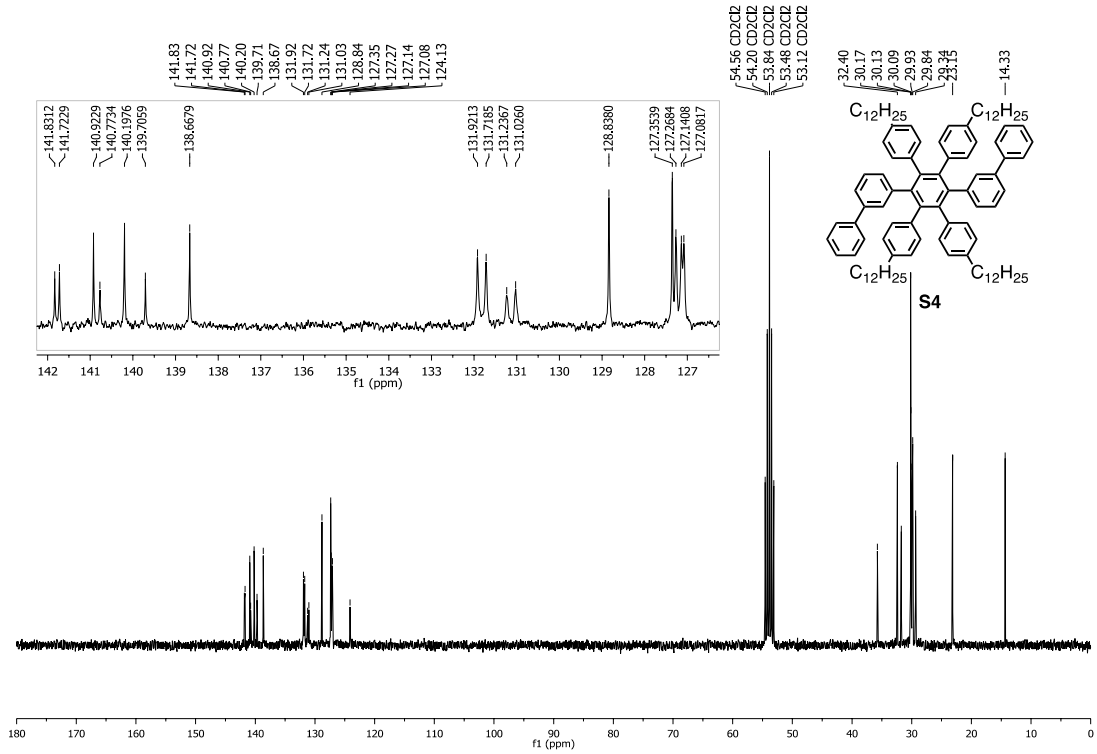
C12H25
S4
f1 (ppm)

3. Investigation of a model system

In order to investigate the efficiency of the cyclodehydrogenation from polyphenylene precursor **6** to GNR **1**, model oligophenylene **S4**, which corresponds to a short cutout of precursor **6**, was synthesized as shown in Scheme S1. 1,3-Di(biphenyl-3-yl)propan-2-on (**2**) was first prepared by the carbonylative coupling of 3-(bromomethyl)-biphenyl (**S1**), and then reacted with 4,4'-didodecylbenzil (**S2**) by *Knoevenagel* condensation to give cyclopentadienone **S3**. Subsequent *Diels-Alder* cycloaddition of **S3** and bis(4-dodecylphenyl)acetylene (**S2**) provided oligophenylene **S4** in 59% yield. The cyclodehydrogenation of oligophenylene **S4** was performed with three equivalents of iron (III) chloride for one hydrogen to be removed, and gave a mixture of polyaromatic hydrocarbons (PAHs) **S5** and **S6** as a dark yellow powder.

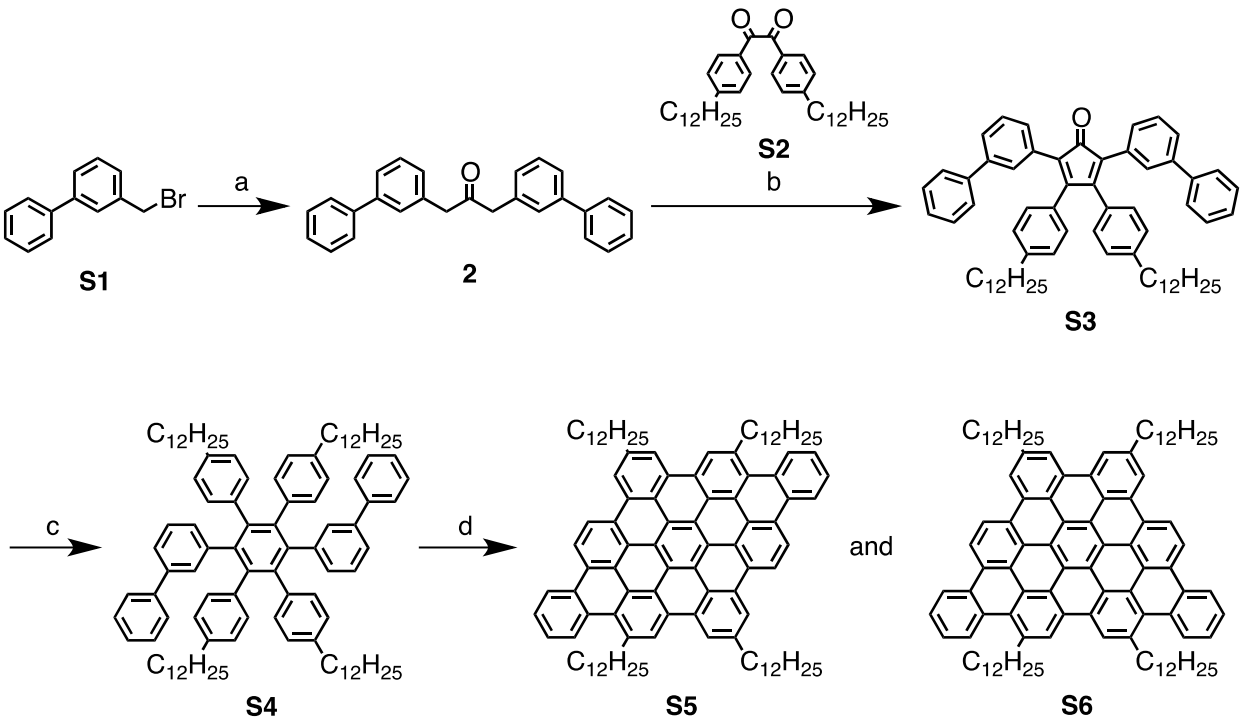

Scheme S1: Synthesis of model compound **S4** followed by cyclodehydrogenation to PAHs **S5** and **S6**; reagents and conditions: (a) $Fe(CO)_5$, benzyltriethylammonium chloride, KOH, CH_2Cl_2/H_2O (19:1), reflux, 41%; (b) tetrabutylammonium hydroxide, *t*BuOH, 80 °C, 66%; (c) bis(4-dodecylphenyl)acetylene, Ph_2O, reflux, 59%; (d) $FeCl_3$, CH_2Cl_2/CH_3NO_2, rt, 72%.

MALDI-TOF MS analysis proved the efficient conversion of oligophenylene **S4** into PAHs **S5/S6** without any partially fused species as evidenced by the isotopic distribution in perfect

agreement with the simulation (Figure S1). Although **S5** and **S6** could not be distinguished by MALDI-TOF MS due to the exactly same mass of the two PAHs, ^{1}H NMR analysis at 120 °C in 1,1,2,2-tetrachlorobenzene-d_2 elucidated the existence of two isomers, **S5** and **S6**, in ca. 1:1 ratio based on the four independent peaks from α-CH_2 protons at δ = 3.82, 3.68, 3.22, and 3.08 ppm with almost the same values of integration. ^{13}C NMR could not be measured even at elevated temperatures and the combination of ^{1}H-^{1}H-COSY and NOESY measurements did not allow the unambiguous assignment of the aromatic peaks for **S5** and **S6**, but the value of integration was consistent with that of **S5** and **S6**, confirming the full cyclodehydrogenation of oligophenylene **S4**. These results indicate that such oligophenylene structure can be perfectly "planarized" and "graphitized", supporting the highly efficient conversion of polyphenylene precursor **6** into GNR **1**.

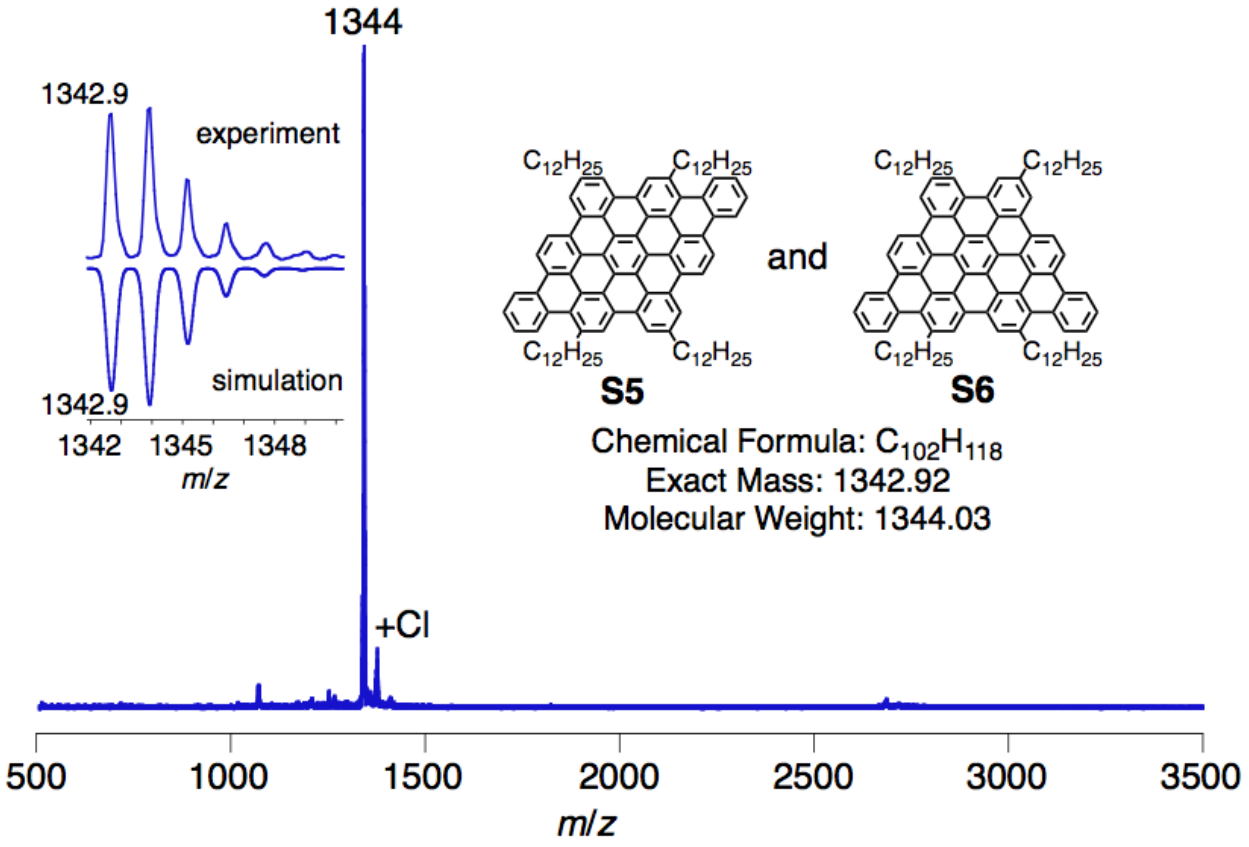

Figure S1: MALDI-TOF MS spectrum of PAHs **S5** and **S6** after the cyclodehydrogenation of precursor **S4**; inset: the isotopic distribution of PAHs **S5** and **S6** in perfect agreement with the simulation.

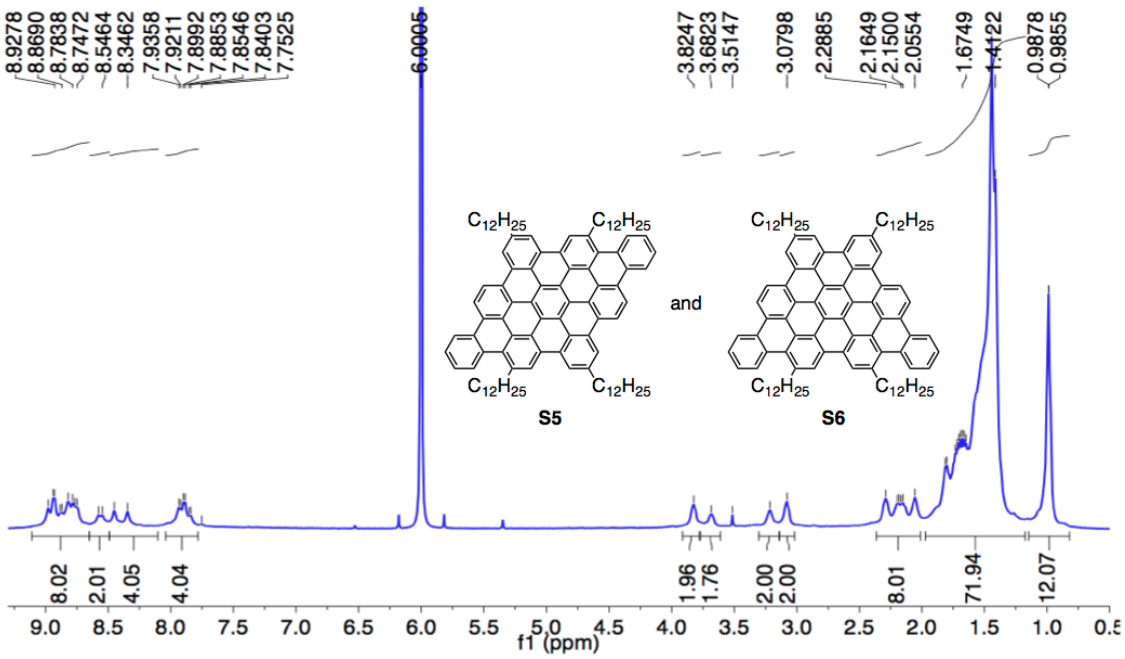

Figure S2: ^{1}H NMR spectrum of the mixture of **S5** and **S6** in 1,1,2,2-tetrachloroethane-d_2 at 120 °C.

4. Characterizations of polyphenylene precursor 6 and GNR 1

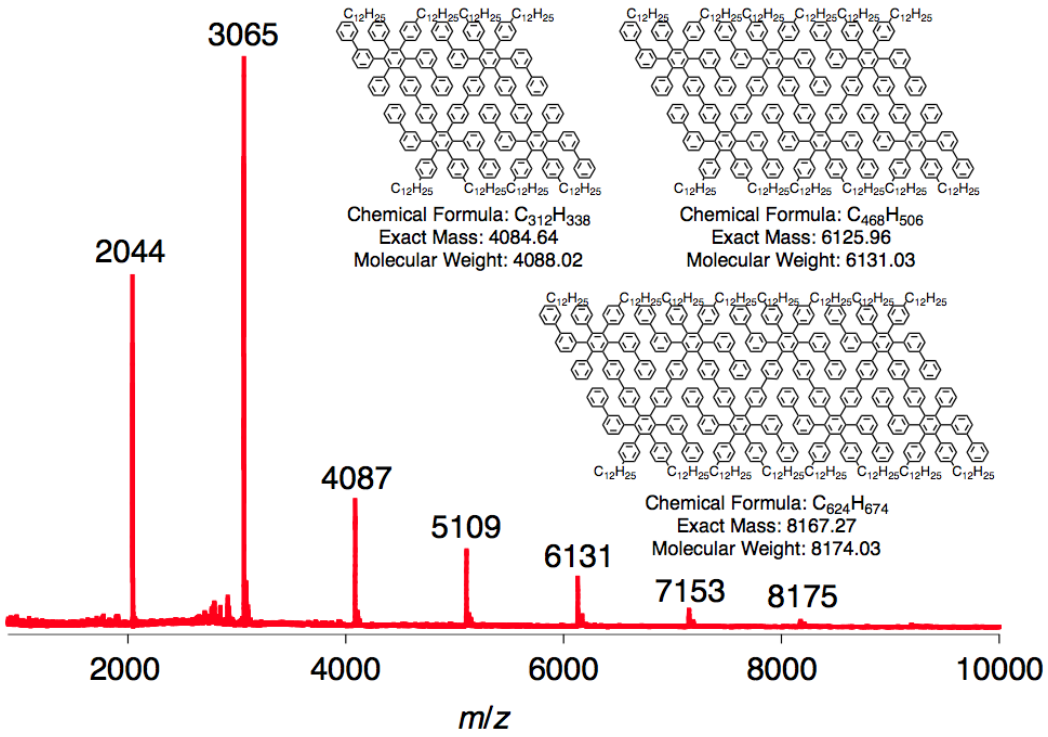

Figure S3: MALDI-TOF MS analysis of polyphenylene precursor **6** (before SEC fractionation, reflectron mode, matrix: TCNQ).

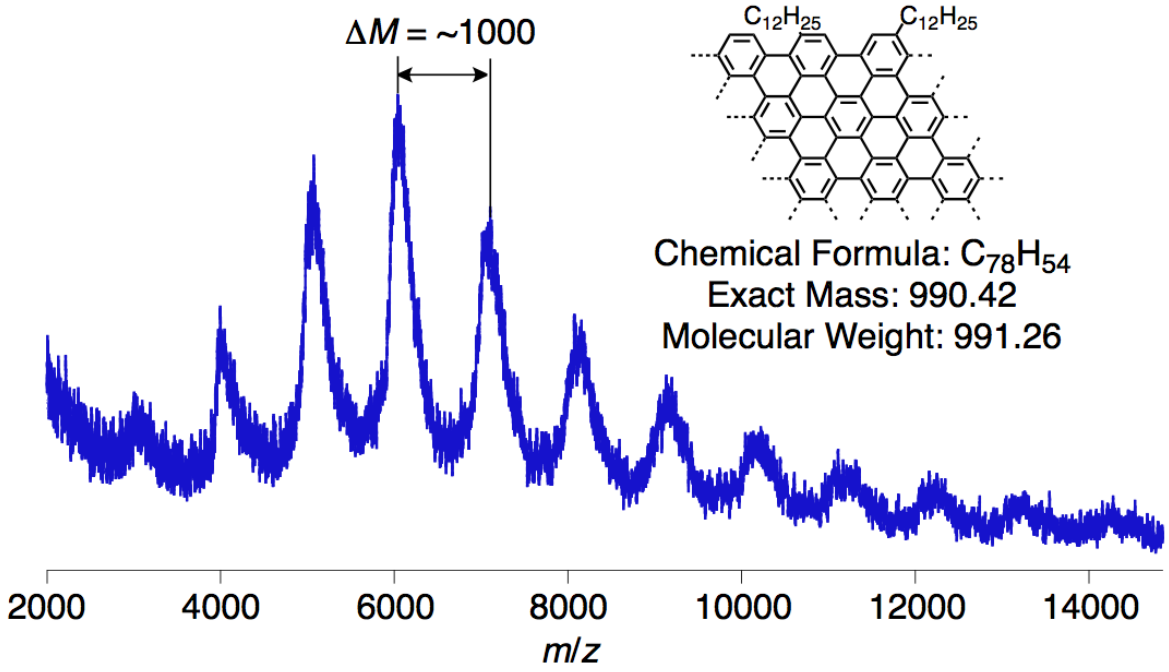

Figure S4: MALDI-TOF MS analysis of GNR **1** (linear mode, matrix: TCNQ).

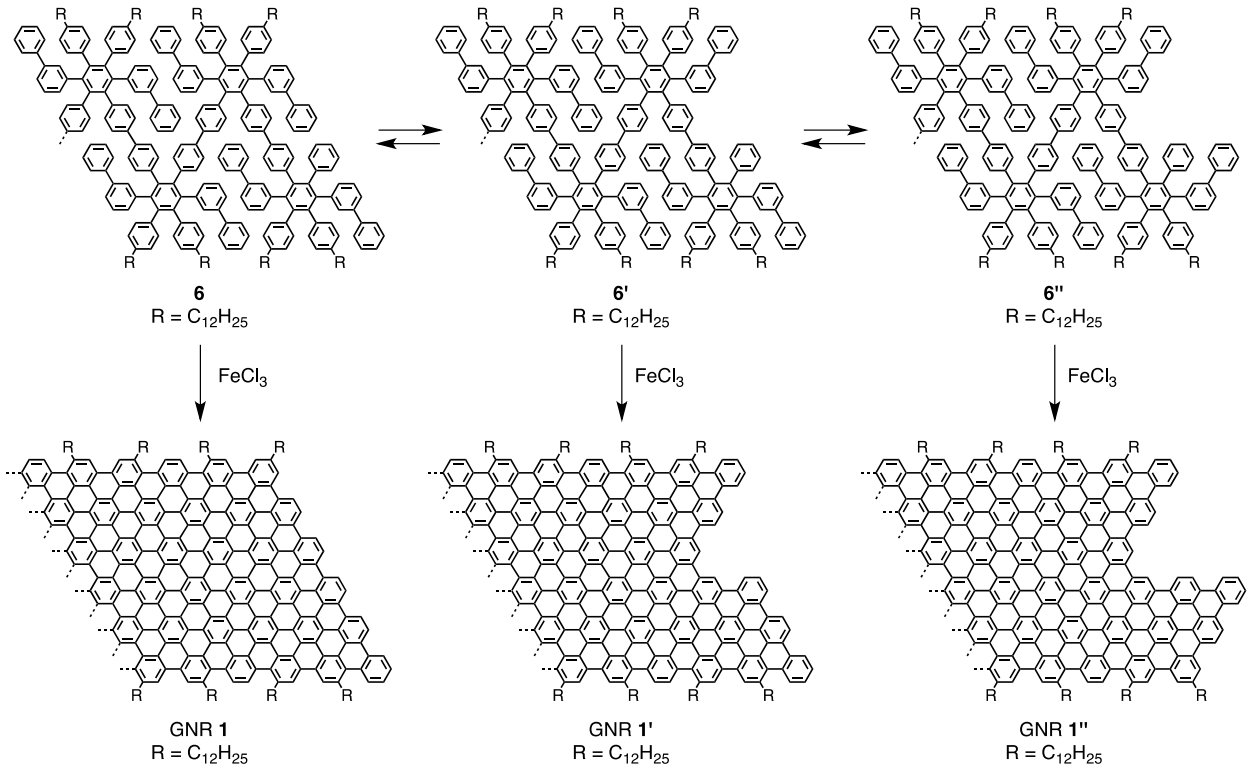

Scheme S2: Structural isomerization at the terminals of GNR **1**.

5. UV–vis absorption spectroscopic characterization of GNR 1

For the UV–vis absorption spectroscopic analysis in dispersion, GNR **1** in *o*-dichlorobenzene (ODCB) with concentration of 0.25 mg/mL was sonicated for 1 h 30 min, then diluted with ODCB by a factor of 5 and placed in 1 cm quartz cuvette. The film was prepared by drop casting GNR **1** dispersion on quartz substrate. The measurements were performed using Jasco V670 spectrophotometer.

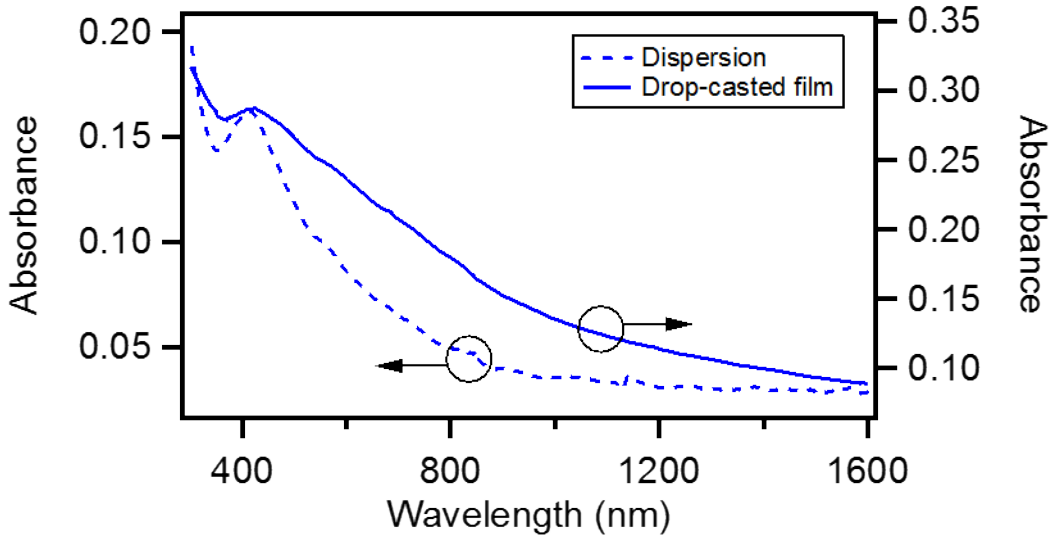

Figure S5: UV–vis absorption spectrum of a dispersion of GNR **1** in ODCB (dashed line) and GNR 1 film (full line)

6. Device Encapsulation

For the Encapsulation, Poly(methyl methacrylate) (PMMA) (120k, Sigma Aldrich) was dissolved in Methyl Ethyl Ketone (MEK) (70 mg/ml). The solution was heated for 60 min at 60°C and then filtered (Carl Roth PTFE 0.45 µm). Subsequently, it was taken inside the glovebox and spin-coated at 1000 rpm for 30 sec on the top of the devices without post annealing.

7. Characteristics in Dark

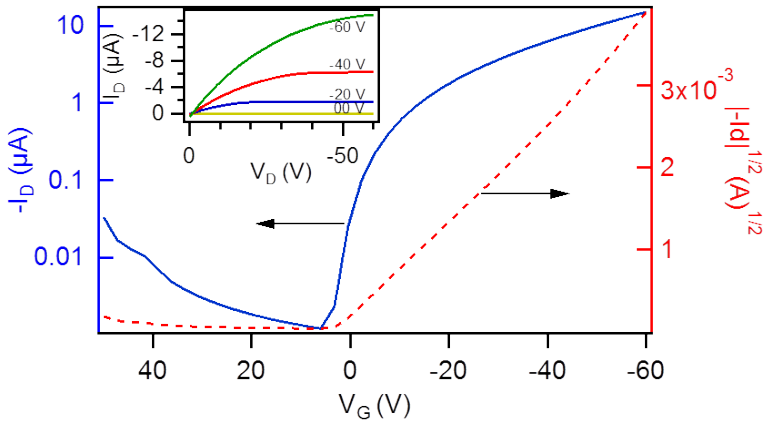

Figure S6 Transfer characteristics of bottom-gate bottom-contact device (***L*** = 120 µm) based on pristine P3HT (left axis in the log scale and the right axis is the square root of the absolute value of the drain current). The inset shows its output characteristics.

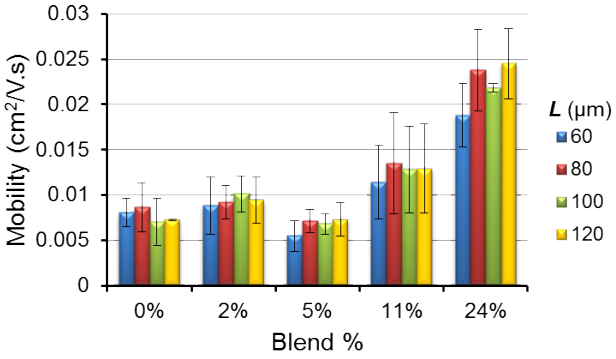

Figure S7: Variation of the field effect mobility with the concentration of the GNRs for the bottom gate bottom contact devices with long channel length (60, 80, 100 and 120 µm).

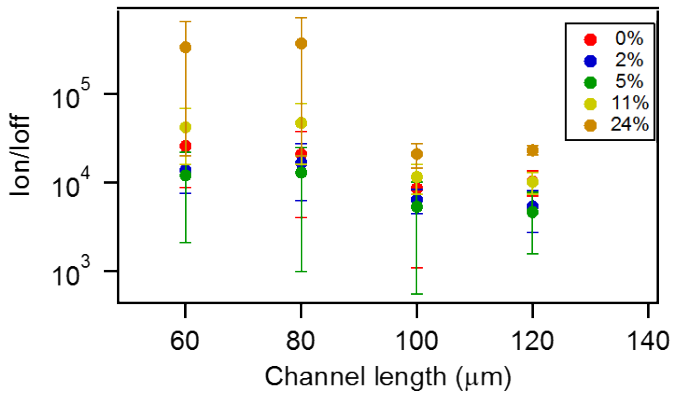

Figure S8 Variation of the I_{on}/I_{off} with the channel length *L=60*, 80, 100 and 120 μm at different blend percentages of GNRs with respect to P3HT.

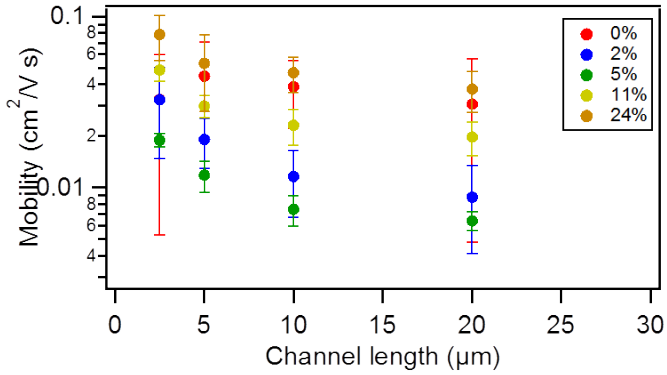

Figure S9 Variation of the field effect mobility (left axis in the log scale) with the channel length (2.5, 5, 10 and 20 μm) at different blend percentages of GNRs with respect to P3HT.

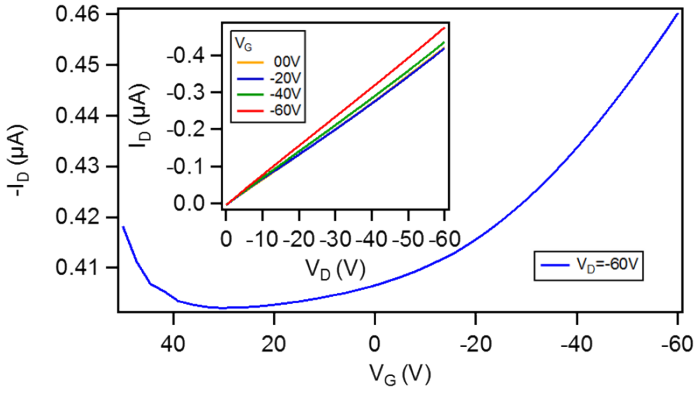

Figure S10 Transfer characteristics of bottom-gate bottom-contact device (***L*** = 20 μm) based on pristine GNRs (prepared by drop-casting (0.25mg/mL in DCB) followed by annealing at 200°C for 15 min). The inset shows its output characteristics.

8. Surface morphology

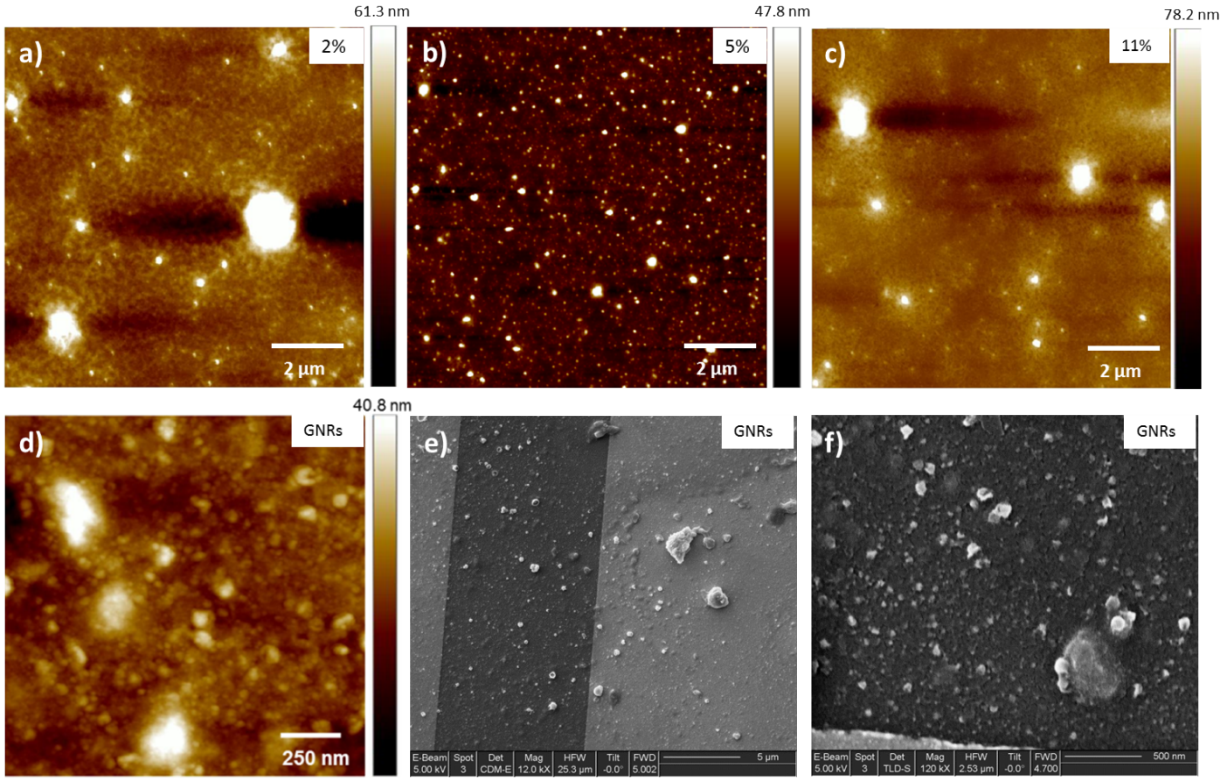

Figure S11 AFM images of films of GNRs with P3HT at a) 2%, b) 5% c) 11%., and d) 0%. e) and f) SEM images for device with pure GNRs (prepared by drop casting).

AFM imaging in tapping mode provides evidence for the increasing presence of large aggregates, featuring sizes on the hundreds of nm, with the increasing quantity of GNR in the blend. Such large aggregates are well monitored in neat GNR films.

9. Sample preparation for UV–vis absorbance measurements

GNRs were dissolved in *ortho*-dichlorobenzene (ODCB) and sonicated for at least 1 h 30 min then immediately transferred to the glove box where they were mixed with a constant amount of P3HT (1.5 mg/mL in ODCB) at different percentages (2, 5, 11 and 24 wt % with respect to P3HT). Thin films were prepared inside the glovebox (N_2 atmosphere) by spin-coating the solutions at 1200 rpm for 60 sec onto quartz substrates (cleaned by Piranha rinsed with water, ethanol and dried with nitrogen). This was followed by an annealing step at 200 °C for 15 min.

Measurements were carried out using Shimadzu UV-3101PC spectrophotometer

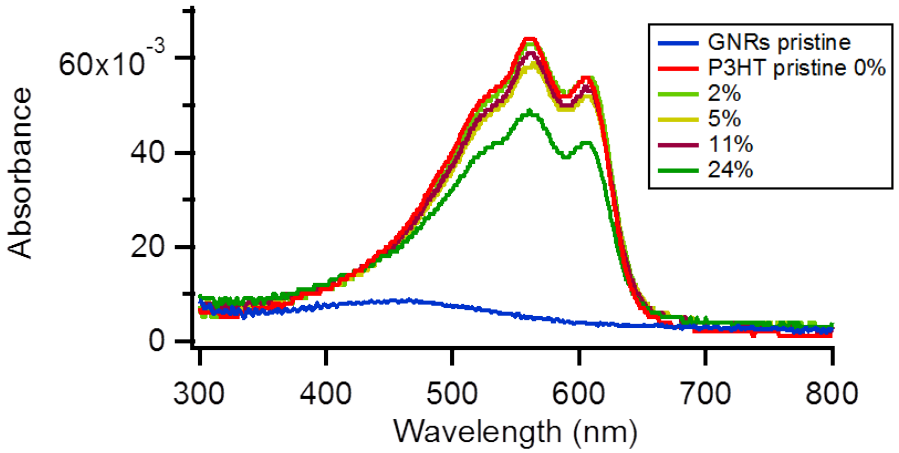

Figure S12: UV–vis absorbance spectra for films of pristine P3HT, GNRs and the blend of GNRs with P3HT at different percentages.

10. Photoresponse

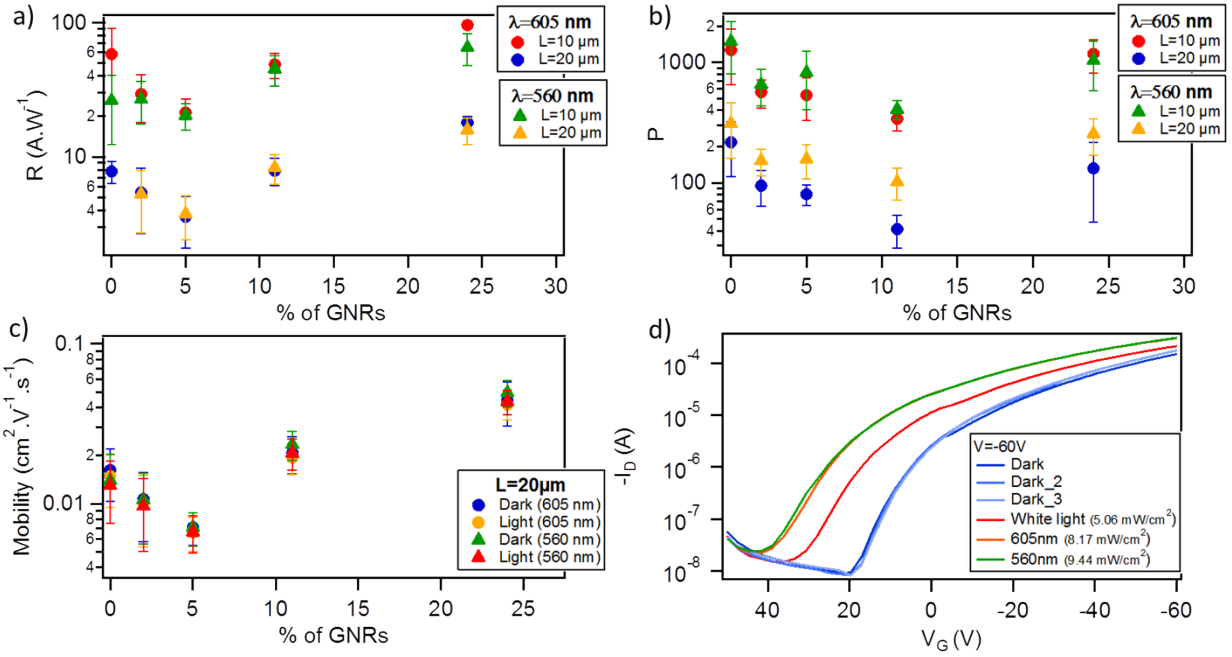

Figure S13 Comparison between: a) Responsivity and b) Photosensitivity for 2 channel lengths (L = 10, 20 µm) OFETs based on different blend percentages of GNRs with respect to P3HT; of these devices at V_D = –60 V under illumination with monochromatic light at two different wavelengths (λ = 605 nm; 8.17 mW/cm^2) and (λ = 560 nm; 9.44 mW/cm^2). c) comparison between the field effect mobility of L = 20 µm devices based on different blend percentages of GNRs with respect to P3HT measured in dark and under illumination with monochromatic light at two different wavelengths (λ = 605 nm; 8.17 mW/cm^2) and (λ = 560 nm; 9.44 mW/cm^2). d) Transfer characteristics at V_D = –60 V of a pristine P3HT device (L = 20 µm) measured in dark, under monochromatic lights (λ = 605 nm; 8.17 mW/cm^2 and λ = 560 nm; 9.44 mW/cm^2) and under white light (5.06 mW/cm^2).

In the main text it is mentioned that "the use of a monochromatic light source with a wavelength matching the peak of absorption of the semiconductor is expected to result in a higher photoresponse as compared to the use of a broad band illumination". To prove that, we picked 2 pristine P3HT devices of $\boldsymbol{L}$ = 20 µm which were investigated under monochromatic light at λ = 560 and 605 nm and we measured the photoresponse under white light (5.06 mW/cm^2) following exactly the same procedure adopted for the measurements under monochromatic light. The results are shown in figure 4d and as expected under illumination with white light, the photoresponse is lower and consequently lower $\boldsymbol{P}$ (59) and $\boldsymbol{R}$ = 6.23 A·W^{-1} values were obtained as compared to the illumination under monochromatic light where $\boldsymbol{R}$ and $\boldsymbol{P}$ were 355 and 7.9 A·W^{-1} at λ = 605 nm and 387 and 7.19 A·W^{-1} at λ = 560 nm respectively.

11. References:

[1] S. Ito, M. Wehmeier, J. D. Brand, C. Kübel, R. Epsch, J. P. Rabe, K. Müllen, *Chem. Eur. J.* **2000**, *6*, 4327.

[2] T. Izawa, E. Miyazaki, K. Takimiya, *Chem. Mater.* **2009**, *21*, 903.

[3] (a) Wasserfallen, D.; Kastler, M.; Pisula, W.; Hofer, W. A.; Fogel, Y.; Wang, Z.; Müllen, K. *J. Am. Chem. Soc.* **2006**, *128*, 1334. (b) Kastler, M.; Pisula, W.; Wasserfallen, D.; Pakula, T.; Müllen, K. *J. Am. Chem. Soc.* **2005**, *127*, 4286.